REMOTE DETECTION OF INSECT EPIDEMICS IN CONIFERS

by

Robert C. Heller 1/

INTRODUCTION

The detection and location of timber lost to destructive agents in the forest is best done by a remote sensing technique of some kind. Most stress, whether it be caused by insects, disease, soil salinity or water deficiency, causes a change in foliage color. This discoloration can be seen better from an aerial platform than by making systematic ground surveys. Some of the early insect surveys by Forest Service entomologists showed that there was more than a 100 times improvement in efficiency by using aerial observation methods as compared with ground methods. Later work has shown still greater improvement in detection success by using color photography at medium scales (1:8,000).

Bark beetles are one of the nation's most serious killers of coniferous timber. Beetles also induce stress faster than any other damaging agent--excluding fire. In the Black Hills of South Dakota there has been a continuing epidemic of the Black Hills beetle *(Dendroctonus ponderosae,* Hopk.*)* in ponderosa pine *(Pinus ponderosa,* Laws.*)*. The Black Hills (Fig. 1) extend about 64 by 160 kilometers and are covered mostly by ponderosa pine. In this vast green area, beetle attacks and associated blue stain fungus cause the affected trees to change color from green to green-yellow, yellow, and yellow-red as the season progresses. Figure 2 is an example of the

---

1/ Pacific Southwest Forest and Range Experiment Station, Forest Service, U. S. Department of Agriculture, Berkeley, California

high contrast in August between healthy trees and those dying from bark beetle attack. A bare area in the foreground of this photograph is a tailings pile caused by gold mining at the turn of the century in the Black Hills. This pile of bare earth measures 80 meters (250 feet) and can be used as a point of reference for the reader when viewing the sample multiscale photographs described later.

I would like to describe two facets of our stress studies in this report--aerial photography and multispectral sensing for previsual detection. In connection with aerial photography, we are interested in optimum combinations of films, filters, and scales which are most effective in detecting stressed-discolored timber. Because the discolored infestations shown in Figure 2 vary in size from 3 to 200 meters, we are afforded natural resolution targets of varying sizes. By obtaining small-scale photographs from our own aircraft and by the NASA RB-57, we were able to study the effect of film and scale on resolution and the expected detectability on ERTS imagery. The second facet of our work involves previsual detection of stressed pine trees. In this case, we would like to determine the best sensor for detecting trees which are infested and dying but which have not yet discolored. If this phase of the work is successful, it will permit timber managers to greatly reduce their cost of insect control measures by permitting them to locate beetle-infested trees, remove them from the woods, and reduce the likelihood of an epidemic continuing and of additional resource losses.

SEASONAL, FILM, AND ALTITUDE EFFECTS ON INFESTATION DETECTION BY AERIAL PHOTOGRAPHY

SEASONAL AND FILM EFFECTS

While bark beetles induce stress more rapidly than most other destructive agents, the slowdown of the tree's metabolism usually requires about nine months before any visible signs of foliage discoloration begin in the Black Hills. For example, when adult beetles attack pine trees in August, it requires almost a full year for new broods to develop and emerge from those trees. The rate at which the trees die depends upon several factors, such as the number of beetles attacking, amount of blue stain fungus development within the xylem, and the susceptibility and vigor of individual pine trees. The drying out of pine foliage is what causes visible discoloration--chloroplasts die and other pigments--carotin and xanthophyll--become visible. Usually a ground observer cannot see the change in foliage color until almost nine months after beetle attack. This is usually in May in the Black Hills. In the South the rate of foliage discoloration from the southern pine beetle can occur in six weeks during the summer months.

We monitored several infestation spots by taking color and color infrared aerial photographs once a month from May through August (Figs. 3A and 3B). From our ground inspection of this site we know that 40 trees of the more than 200 tree images in these photos have been attacked; this infestation measures 36 meters (120 feet) in diameter. In May, only about 10 trees are visible on either the color or color infrared photos; the lighter yellow trees on the color photo (Fig 3A) are those which are

beginning to discolor first. On the color infrared (Fig 3B) in May, the same trees appear as a lighter pink. More and more trees discolor as the season progresses through June, July, and August. In August, all 40 trees were visible and detected by the photo interpreters. As a result of these studies we have found that color or color infrared film does not act as a previsual sensor. These films, then, are useful for detecting discolored trees only. We also learned that maximum contrast and maximum discoloration occurred in August.

ALTITUDE AND RESOLUTION EFFECTS

The Earth Resources Technology Satellite (ERTS) is expected to be put in orbit in March 1972. While no one can predict exactly the kind of spectral response and resolution qualities that the return-beam vidicon and four-channel multispectral scanner will produce, the expectations are that resolution will probably be no better than 100 meters. In August 1969, we attempted to obtain aerial photography of vegetative stress which closely approximates the spectral band widths which will be used on the television camera or multispectral scanner. These band widths are listed as follows:

Spectral Band Width (micrometers)

Channel or Camera	Multispectral Scanner	RBV Camera
1	0.5 - 0.6	0.475 - 0.575
2	0.6 - 0.7	0.580 - 0.680
3	0.7 - 0.8	0.690 - 0.830
4	0.8 - 1.1	

While not all of the filters used in aerial photography coincide with the multispectral scanner channels or the RBV cameras, some of the Wratten filters approximate these spectral band widths. For example, the Wratten 58 filter is close to the first channel of the multispectral scanner and the first camera of the RBV, and the A25 Wratten filter approximates channel 2 and camera 2 of these ERTS subsystems. Similarly, the Wratten 89B filter used with infrared aerial film approximates channels 3 and 4 of the multispectral scanner and the third camera in the RBV subsystem. These combinations of filters and other color films were requested to be flown from the RB-57 aircraft in August 1969. The actual cameras and filters flown on this flight are listed in Table 1.

RB-57 Flight - Mission 101

Two flights were made by the RB-57--one on August 3, and the second on August 8, 1969. Photographs from the August 3 flight were not usable because the area was more than 80 percent cloud covered. The plotted flight lines of the August 8 flight are shown on Figure 4. Three flight lines were requested to be flown which cover the northern part of the Black Hills National Forest. This figure shows the actual location of the flight lines flown on both August 3 and August 8. Unfortunately, the predicted flight line location did not coincide with the actual location, and we were unable to get the coverage desired. Flight line orientation within the Black Hills is particularly difficult because of lack of landmarks; if any future high-altitude flights are made, we would suggest extending

the beginning and ending points of the flight lines so that flight line location is properly identified.

The purpose of the requested RB-57 coverage was to make a comparison of color photography taken at a scale of 1:8,000 at predetermined flight strip locations throughout the northern Black Hills. We had hoped to develop a relationship between 10 sample strips (1.6 by 16 kilometers) covered by large-scale (1:8,000) color photographs and the RB-57 color and color infrared photographs (1:110,000). The estimates of mortality derived by using probability sampling from the large-scale color photography strips are reported by Heller and Wear (2). Examination of the flight map (Fig. 4) shows that only four of the ten large-scale strips were covered by all scales of the RB-57 flight.

We fortunately obtained complete large- and small-scale photographic coverage of a 1.6 by 6.0 kilometer study area (Fig. 5) which contained 211 discolored infestations (or variable-size resolution targets). The sizes of each infestation were measured carefully on the ground, located on aerial photographs, and the numbers of trees counted within each infestation. Data from this ground survey, then, were used to rate photo interpretation efficiency. All subsequent sample photography can be oriented to this study area; the gold mine tailings pile described earlier in Figure 2 can be seen in Figure 6 which is representative of the Zeiss color photography (1:8,000) taken along our sample strips. Only the portions of the 9-inch format photography (Zeiss 12-inch focal length and RC-8 6-inch focal length cameras)

which cover the study area are shown in Figure 7. Similarly, examples of 3 of the Hasselblad photos are shown in color, infrared color, and color film taken through a minus blue filter in Figure 8; they also cover the same study area.

Almost all RB-57 aerial photography exposed over the Black Hills was underexposed from one to one-and-one-half diaphragm stops. This was true for all large-format photography and for four of the six Hasselblad cameras. The only properly exposed films were the color film exposed through the minus blue filter and the Ektachrome infrared film with the Wratten 15 filter with two of the Hasselblad cameras. Reflectance can be two to four times lower over a dense forest as compared with open farm land which surrounds the Black Hills. Exposures over farm land looked quite good. We would suggest the installation of automatic exposure controls on the diaphragms of all NASA cameras since it is impossible to make manual diaphragm adjustments once the RB-57 leaves the ground. Underexposure causes the duplicate transparencies to be excessively dark; small targets are not resolved, and shadows along north-facing slopes are so dark that even high-contrast targets are obscured. Thus, definite conclusions on best film, filter, and scale combinations are difficult to determine from these particular photographs.

Despite the fact that most of the film was underexposed, we interpreted all images over the study site. As might be expected, the larger the scale, the greater the accuracy. Also, as the infestations or targets became larger, the infestation accuracy improved (Fig. 9).

In comparing the films used on the Hasselblad cameras, all at a scale of 1:220,000, we obtained a similar trend as far as infestation size is concerned (Fig. 10). In this case the films which rated the highest were the color infrared, the color film with the minus blue filter, and the Panchromatic film with a 25A filter. The color film with a minus blue filter rated fairly high probably because it was one of the better exposed films of the lot.

The results of our own moderately small-scale photography over the study area compares just two color films (color and false color), but by infestation size in meters (Fig. 11). Again, as infestation size (or resolution size) becomes large, detection success improves; however, detection success is acceptable only on the larger infestations (over 30 meters in size and more than 20 trees) when scales as small as 1:174,000 are used. For determining stress in the early stages of an epidemic, it is apparent that we will need good resolution capabilities--probably 5 meters (16 feet). For discovery of stress in very remote areas, we may be able to detect discolored timber with resolution capabilities of 30 to 50 meters (100 to 200 feet). Based on the expected resolution (100 meters) of the two ERTS sensors--the return-beam vidicon and four-channel line scanner--it seems unlikely that we will be able to detect any but the largest discolored areas.

PREVISUAL DETECTION WITH MULTISPECTRAL SCANNERS

BIOPHYSICAL MEASUREMENTS TAKEN ON HEALTHY AND INFESTED TREES

A great many techniques were developed and improved over the course of this study. Most of these methods have been described in detail by Weber (5) and Heller (3), but the ones which have been added during the past year and which have helped us derive our ground truth information more quickly are listed below:

Soil moisture data are now being collected by a neutron probe (Fig. 12A). This device measures a differential bombardment of neutrons from a nuclear source through moist and dry soils to a detector. It replaces the Coleman soil moisture meter which we had used previously.

Solar radiation and net radiation will now be monitored by aerial tramways which travel above the tops of the trees on wires supported between tall towers (Fig. 12B).

In the early stages of our study, most of the data were collected independently on separate recording instruments and analyzed separately--a slow, tedious process. In 1970, we used a data logger and the moving tramway described by Wear and Weber (4) on their *Poria weirii* study to collect up to 38 channels of data, digitize them, and store them on magnetic tape (Fig. 12C). This system, now being erected on the Black Hills test site number 149, permits rapid access to the data and is in computer-compatible form. It saves up to one year on the analysis of the energy budget data. Now we can log internal needle temperatures, net and total

radiation, and wind velocity and direction continuously. We have developed computer programs which will recover these data the day after they are recorded.

Optical-mechanical Scanning Imagery

In a NASA-sponsored flight in July 1969, the University of Michigan multispectral line scanner was flown over our instrumented test site (number 149). It used the discrete channels shown in Table 2. Data were collected at four time periods--early morning, midmorning, early afternoon, and late afternoon. These periods coincided with maximum change in tree metabolic activity as determined from our field measurements. We used handy-talky radios for ground-to-air communications, primarily to inform the operator of the thermal scanner about the range of apparent temperatures in ground targets. This information permitted him to adjust his temperature-controlled reference plates on the thermal line scanner.

We received analog printouts of each of the channels listed in Table 2 about one month after the July flight. Because our target size is relatively small for training the processor in the tape-loop training system of combining channels, we had to devise special adaptations of programs developed by Hasell, Le Gault, and Thomson (1).

Our training sets consisted of four classification models--healthy ponderosa pine, nonfaded infested ponderosa pine, discolored and dying ponderosa pine, and old-killed trees. In using the SPARC (Spectral Processing and Recognition Computer) processor and associated digital

computer, we first determined the optimum channel selection for the above four classifications. We found that little improvement of channel combining beyond five channels occurred and that the 0.8 to 1.0 micrometer meter band was the most efficient band in separating pine trees from all other classes of targets. The 0.40 to 0.44 spectral band was the most efficient in separating the old-killed trees from healthy and green infested trees.

Both the maximum likelihood ratio analysis and Euclidian distance analysis techniques were used at several voltage threshold levels. The combined target signature transparencies were made into color Ozalids to produce color mosaics for the selected flight periods during the day. We received the processed data from the Willow Run Laboratories in November 1970.

Several attempts were also made to separate targets by "thermal contouring". In this processing technique, one can adjust a limited temperature range of objects so that they may be expanded over a wide gray scale range. Since flights were made at three altitudes above terrain (450, 900, and 1350 meters), we were able to process the best single flight run for each altitude. The selection of the best flight run was done very carefully and only after consideration was given to the maximum temperature ranges between the healthy and affected trees occurring on the ground at the time of the flight. Figure 13 is an example of a 17° C. (Celsius) spread of target temperatures which occurred on July 22 at 1325 hours; this was a 900 meter-altitude flight using the 8.2 to 13.5 micrometer waveband. This color mosaic was compared carefully with the 1:8,000 scale color photographs taken

with a Zeiss camera over the study area. There is good agreement on many of the general classifications such as separation of grass from hardwoods, from pure conifers, and from exposed rock and soil. Some of the affected pine trees were confused with the nonaffected, but in general, classification accuracies are much improved over what was done one year earlier.

An example of the complex physical and biophysical factors which affect the emission of healthy and insect-infested trees can be seen in Figure 14. Note particularly the third graph down from the top where emission temperatures are shown. On this particular day, the greatest difference in temperature occurred between the healthy and attacked trees about 1500 hours; however, measurable differences began to show up after 1200 hours. In general, ground emission temperatures have been fairly sizeable--2° to 6° C. (Celsius)--on bark beetle-attacked trees. However, we have not been able to show a marked temperature difference for Douglas-fir trees infected with a *Poria weirii* root rot disease in Washington. A similar graph of data has been made in the disease case on two dates--May and July 1970 (Fig. 15); note again that the emission temperatures of the infected and healthy Douglas-fir trees are almost identical. It is therefore unlikely that any kind of thermal sensor would be successful in detecting the differences between these two classes of trees. A digital gray map was made from the analog scanner data at the University of Michigan and is shown in Figure 16. The objects on this gray map which are warm appear darker in tone; the cooler trees and shadows are very light in their representation of lower temperatures. Note that there is an almost uniform representation

of temperature of the trees located under the towers where the tramway-collected thermal data were made. These data support the null hypothesis that there is no temperature difference in the case of disease-infected trees, and therefore sensing with an airborne thermal scanner would be useless, at least in the case of *Poria weirii* (Fig. 16).

CONCLUSIONS

1. With properly exposed color or infrared color film, we can expect to detect discolored foliage caused by insect infestations in ponderosa pine on moderately small-scale photographs (1:32,000) with acceptable accuracies of all but the smallest infestations--less than 6 meters in diameter.

2. Black and white photographs taken from the RB-57 with Hasselblad cameras which matched the wavebands of the ERTS multispectral scanner were combined into one additive color photo. This imagery was not as useful as photographs taken on color, color infrared, or color film with a minus blue filter. Underexposure of the black and white Hasselblad imagery is the probable reason for this.

3. Based on the high-altitude color and color infrared photos which we have obtained to date, it is likely that only insect infestations larger than 100 meters in diameter will be detectable on ERTS imagery.

4. Multispectral preprocessing and processing procedures developed at the Willow Run Laboratories of the University of Michigan have improved over the past year; however, SPARC-processed data from the multispectral

scanner indicate that there are more commission errors than we are willing to accept for accurate detection of beetle infestations.

5. Processing of thermal data by thermal contouring is another technique which shows promise, but it, too, does not discriminate green infested trees from the discolored infested trees to acceptable accuracy levels.

6. It is unlikely that we will be able to improve previsual detection until an instrument is available which combines the thermal, near infrared, and visible channels. We look forward to testing a single aperture multispectral scanner and feel that it will provide us with the most powerful sensing device for previsual detection.

LITERATURE CITED

1. Hasell, P. G., R. Le Gault, and F. J. Thomson. 1968. Investigations of spectrum matching techniques for remote sensing in agriculture. Interim report, Volumes 1 and 2 (Report 8725-13-P). Willow Run Laboratories of the Institute of Science and Technology, University of Michigan, Ann Arbor, Michigan.

2. Heller, R. C., and J. F. Wear. 1969. Sampling forest insect epidemics with color films. Sixth International Symposium on Remote Sensing of Environment Proc. 1969:1157-1167.

3. Heller, R. C. 1968. Previsual detection of ponderosa pine trees dying from bark beetle attack. Fifth Symposium on Remote Sensing of Environment Proc. 1968:387-434.

4. Wear, J. F., and F. P. Weber. 1969. The development of spectro-signature indicators of root disease impacts on forest stands. Fourth Annual Report. Available in microfiche from NASA, Washington, D.C. Scientific and Technical Aerospace Reports.

5. Weber, F. P. 1969. Remote sensing implications of water deficit and energy relationships for ponderosa pine attacked by bark beetles and associated disease organisms. Ph. D. Thesis. University of Michigan, Ann Arbor, Mich. 143 pp. Available in microfiche from University of Michigan.

Table 1. Film-filter-scale combinations exposed during RB-57 Flight Mission #101 - August 3 and 8, 1969.

Film	Filter	Camera	Focal Length	Scale	Format
Color IR (SO 117)	Zeiss "B" (15)	Zeiss	304 mm.	1:55,000	210 mm.
Color (2448)	HF-3	RC-8	152 mm.	1:110,000	210 mm.
Color IR (SO 117)	15	RC-8	152 mm.	1:110,000	210 mm.
Color (SO 368)	2A	Hasselblad	76 mm.	1:220,000	70 mm.
Color (SO 368)	12	Hasselblad	76 mm.	1:220,000	70 mm.
Color IR (SO 180)	15g	Hasselblad	76 mm.	1:220,000	70 mm.
Panchromatic (3400)	58	Hasselblad	76 mm.	1:220,000	70 mm.
Panchromatic (3400)	25A	Hasselblad	76 mm.	1:220,000	70 mm.
Panchromatic IR (SO 246)	89B	Hasselblad	76 mm.	1:220,000	70 mm.

Table 2 Spectrometer channels used for target recognition by University of Michigan aircraft and processing unit and their respective spectral colors

SPECTRAL COLOR	WAVELENGTH (Micrometers)	CHANNEL NUMBER
Violet	.40 - .44	1
	.44 - .46	2*
Blue	.46 - .48	3
Blue-Green	.48 - .50	4*
Green	.50 - .52	5
	.52 - .55	6
Yellow-Green	.55 - .58	7
Yellow	.58 - .62	8
Yellow-Red	.62 - .66	9
Light Red	.66 - .72	10
Deep Red	.72 - .80	11
	.80 - 1.0	12
Reflective Infrared	1.0 - 1.4	13
	1.5 - 1.8	14
	2.0 - 2.6	15
Thermal Infrared	4.5 - 5.5	16
	8.2 - 13.5	17

*Not used in the course of this study.

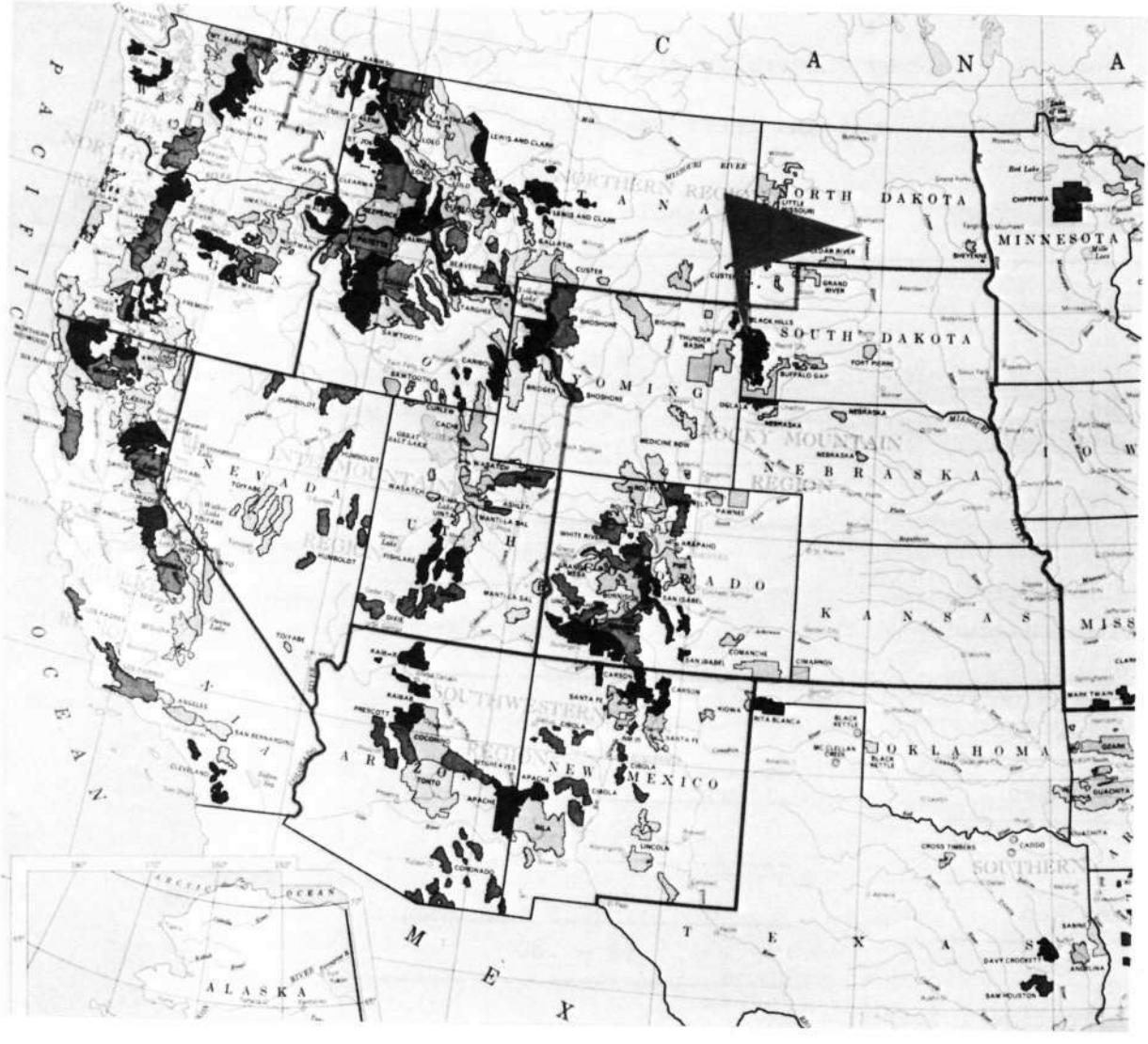

Figure 1.--Flag shows location of Black Hills National Forest near Rapid City, South Dakota.

Figure 2.--Oblique view of Black Hills beetle, *Dendroctonus ponderosae*, Hopk., damage to ponderosa pine, *Pinus ponderosa*, Laws. Yellow to yellow-red trees are most recently killed and offer greatest contrast to healthy pines. Note the mine tailings in foreground; it measures 80 meters (250 feet) and can be seen in small-scale imagery taken by RB-57 (Figures 7 and 8).

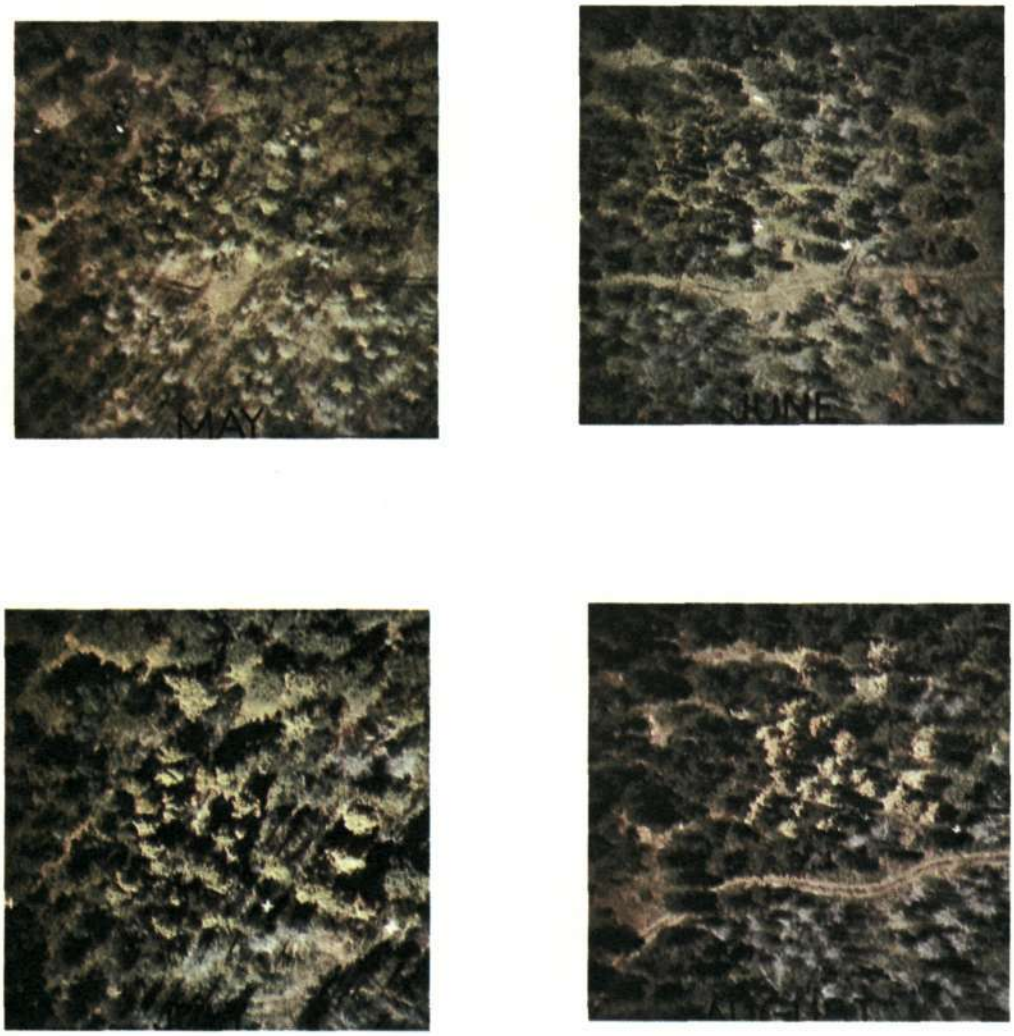

Figure 3A. Normal color film - Anscochrome D/200. Seasonal differences of tree stress caused by bark beetles. Forty infested ponderosa pine trees occur on these transparencies. Note the rate of foliage discoloration in May, June, July, and August--scale 1:1,600.

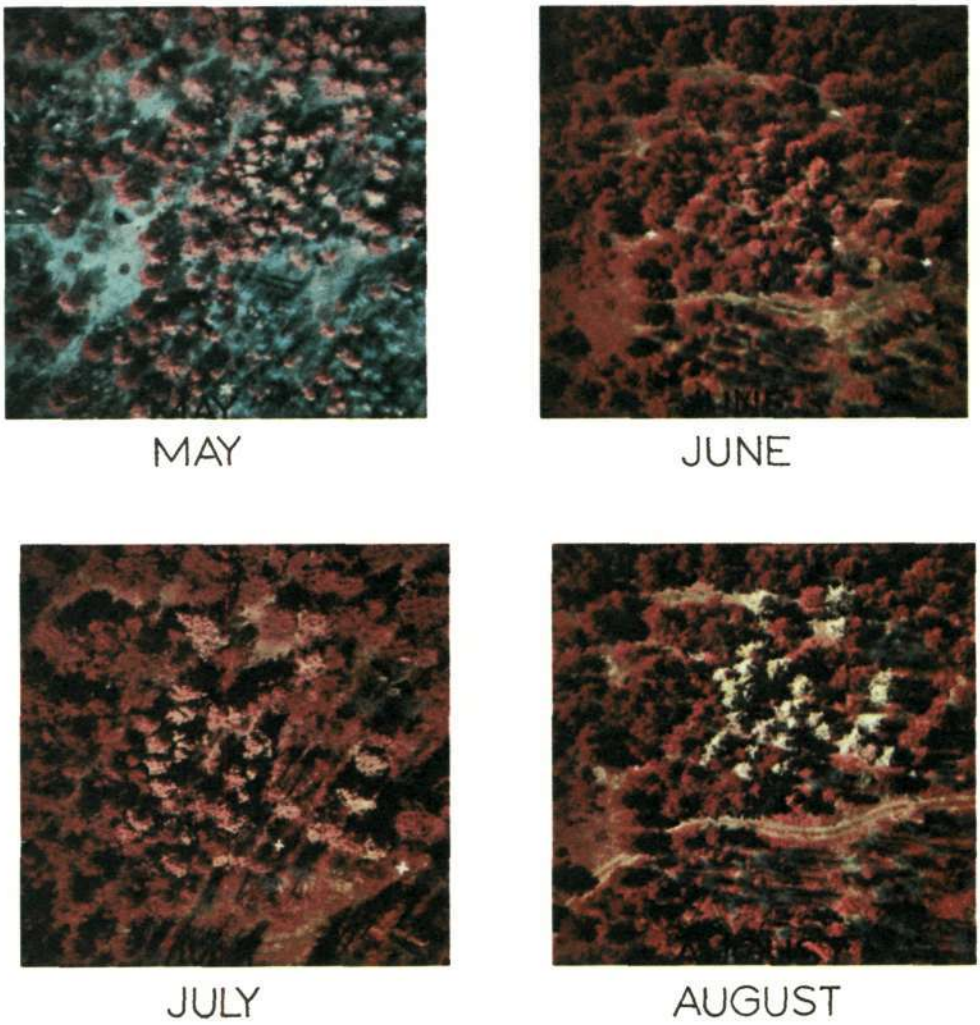

Figure 3B. Kodak Ektachrome Infrared Aero - type 8443. Seasonal differences of tree stress caused by bark beetles. Forty infested ponderosa pine trees occur on these transparencies. Note the rate of foliage discoloration in May, June, July, and August--scale 1:1,600.

CHART OF DESIGNATED FLIGHT LINES AND COVERAGE OBTAINED
BY NASA RB-57 FLIGHT, AUGUST 3 & 8 , 1969.

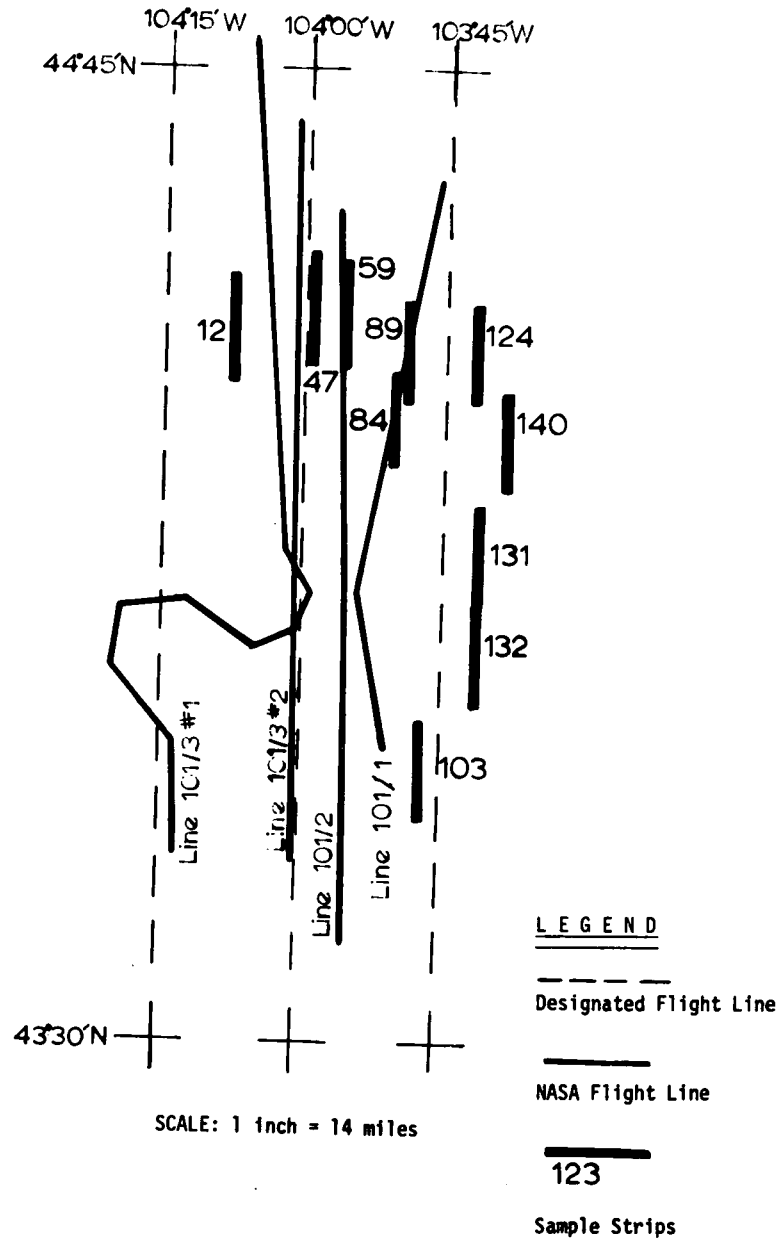

Figure 4.--Flight coverage of RB-57 on August 3 and 8, 1969. Dashed lines show expected flight line location. Heavy lines show 10 samples--each 1.6 by 16 kilometers, taken on color film--scale 1:8,000.

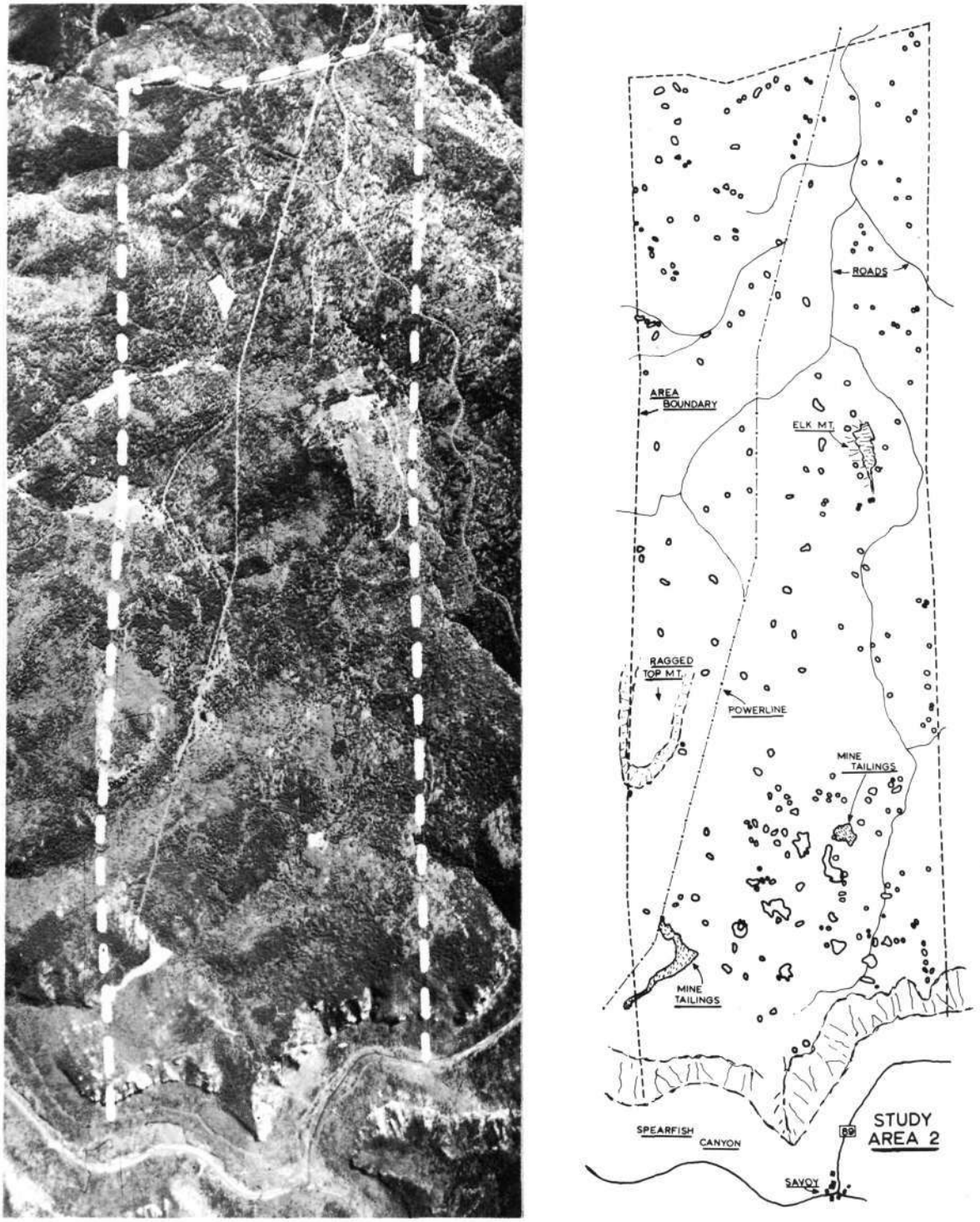

Figure 5.--Aerial mosaic on left of 1.6 by 5 kilometer study area near Lead, South Dakota. On right, 211 infestations of various sizes (3 to 200 meters) are plotted at the same scale.

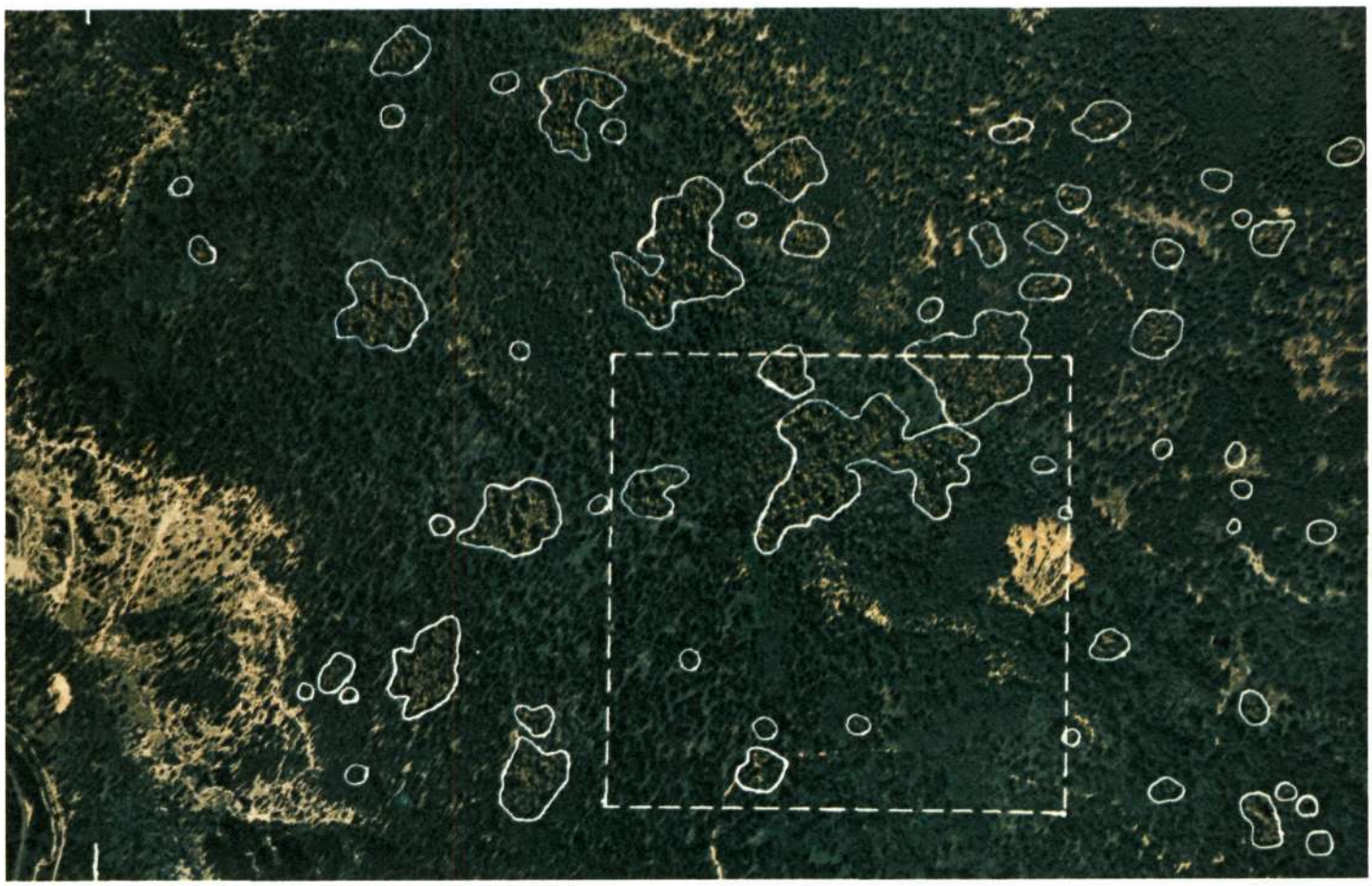

Figure 6.--Color photograph taken on August 11, 1969, with Zeiss 21/23 aerial camera over study area--scale 1:8,000. Infestations are outlined in white. Note high contrast of tailings pile shown on oblique (Figure 2). While several infestations are larger, target contrast is lower because of grassy ground cover.

(A) 1:110,000

(B) 1:110,000

(C) 1:55,000

Figure 7.--RB-57 coverage of study area. (A) RC-8 152 mm. Ektachrome (2448) + HF-3. (B) RC-8 152 mm. Ektachrome Infrared (SO 117) + 15. (C) Zeiss 304 mm. Ektachrome Infrared (SO 117) + "B" (15). Most forested areas were underexposed one to two times.

(A) 1:220,000

(B) 1:220,000

(C) 1:220,000

(D) 1:220,000

Figure 8.--Hasselblad imagery over 1.6 by 5 kilometer study area. Note size of tailings pile (80 meters). (A) Color (SO 368 + 2A). (B) Color IR (SO 180 + 15). (C) Color (SO 368 + 12). (D) Composite infrared photo prepared from the green, red, and infrared black-and-white transparencies; no additional benefits in detection of infestations could be found in this recombination.

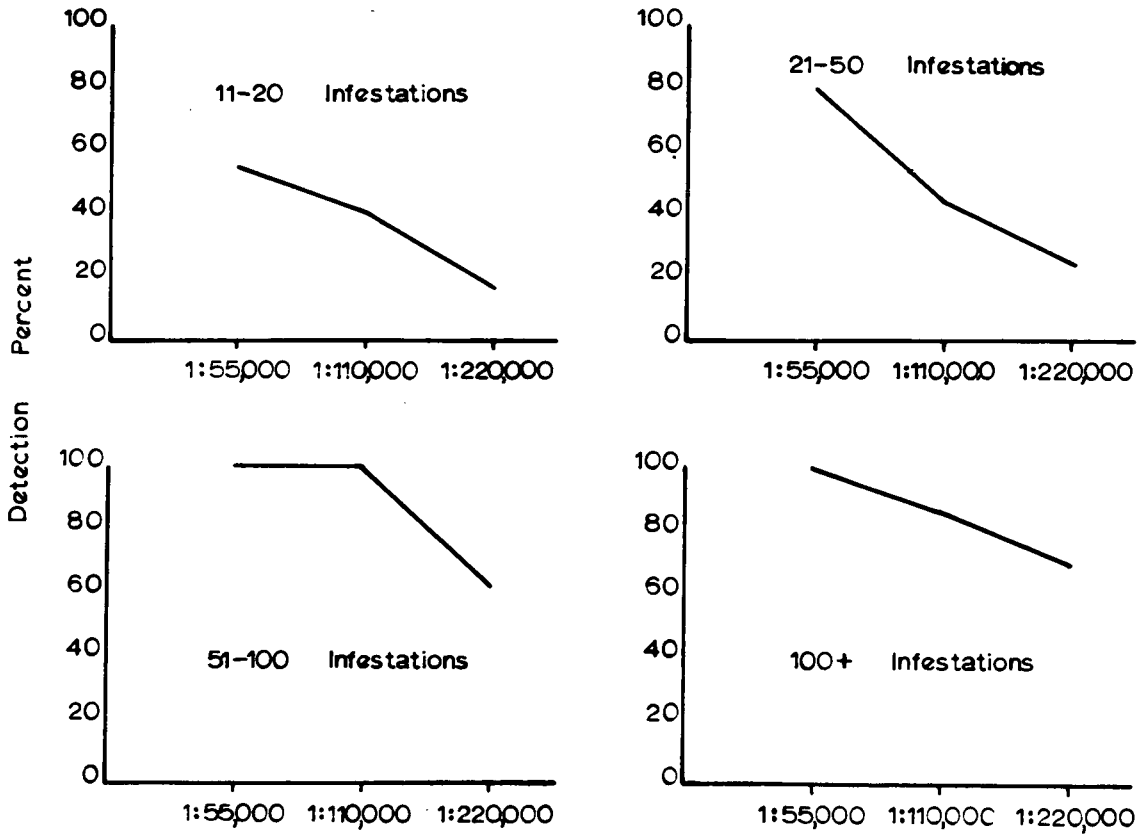

Figure 9.--Detection success in locating infestations on study area by scale and by size of infestation.

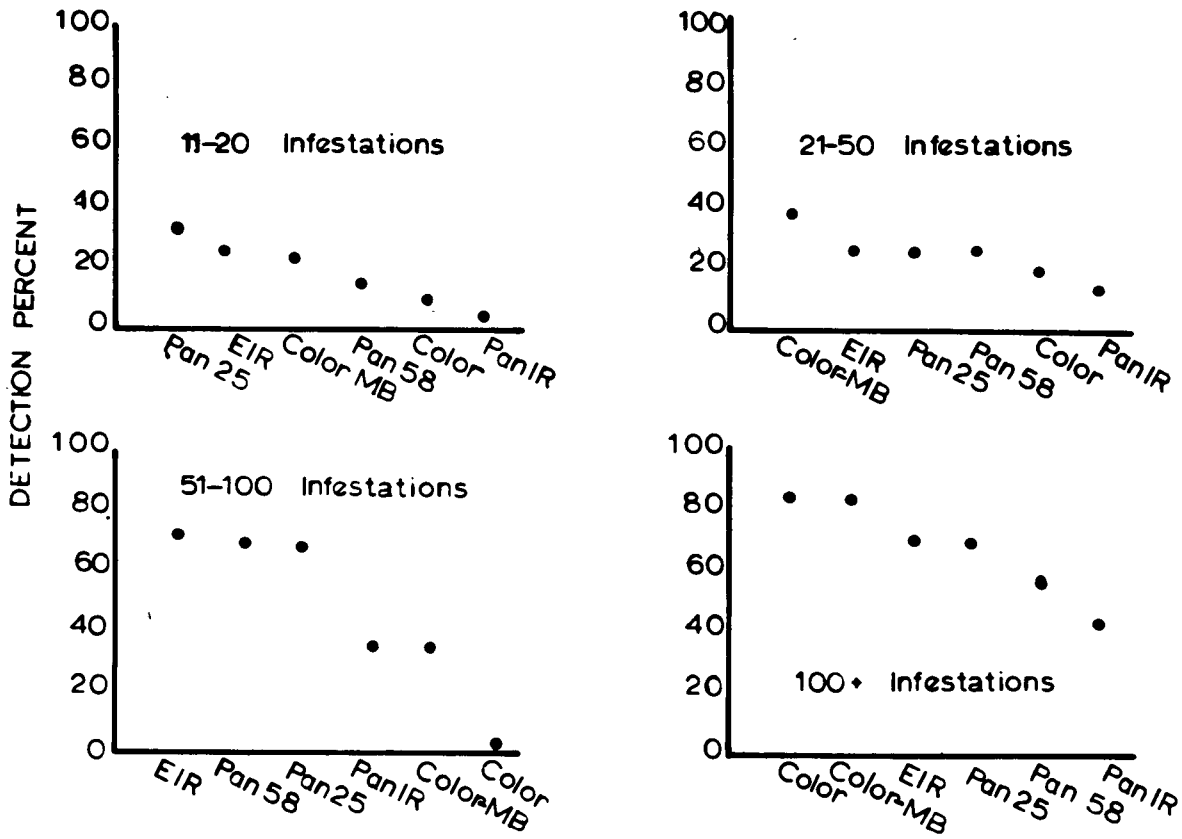

Figure 10.--Detection success in studying various films and filters on 1:220,000 scale Hasselblad photography over 1.6 by 5 kilometer study area.

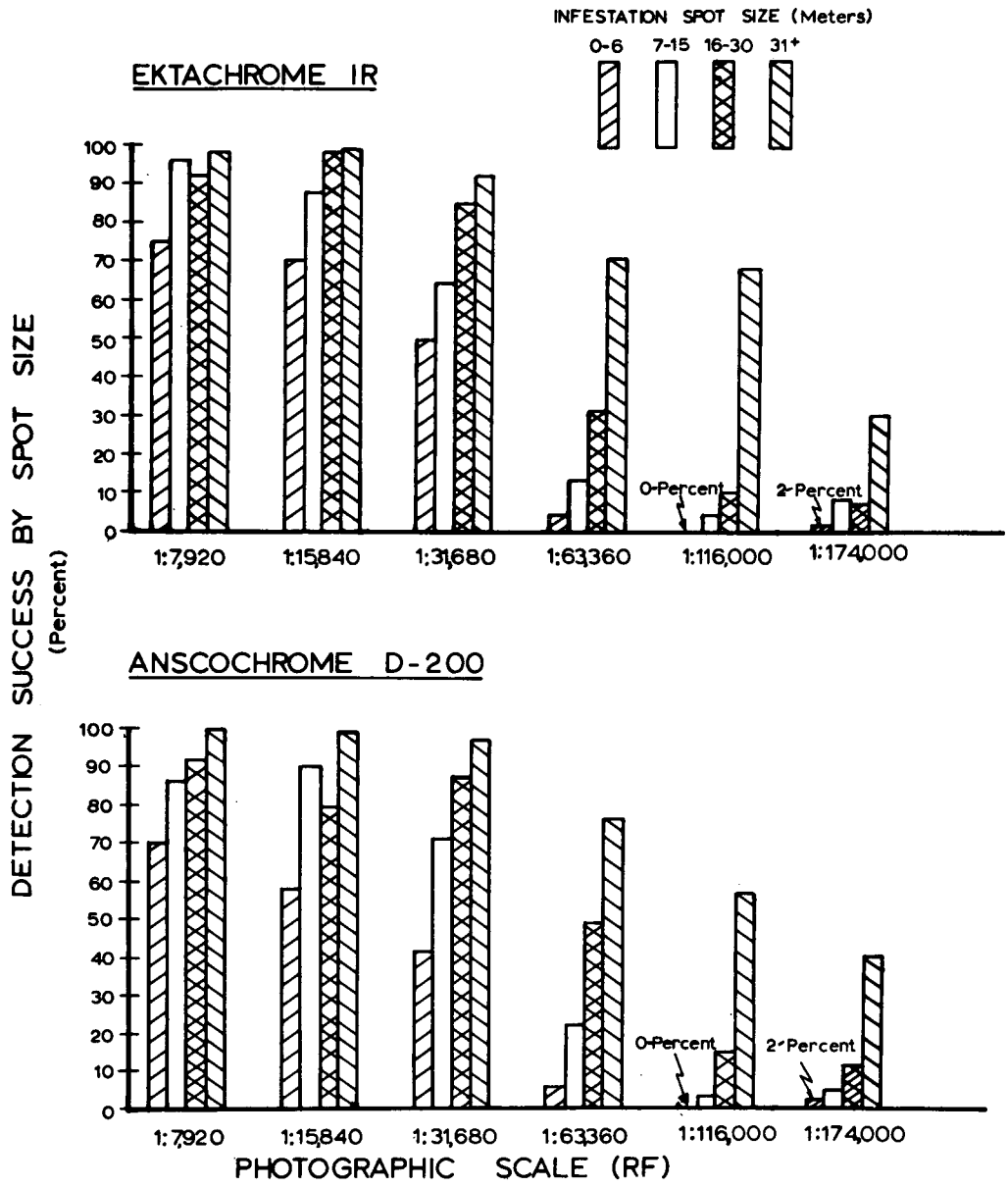

Figure 11.--Photo interpretation detection successes on well-exposed color and color infrared film over study area. Infestations were grouped into four target size classes. Best scale for detection is 1:31,680, but even at 1:174,000 larger infestations can be discerned.

Figure 12A. Improved ground data instrumentation. Neutron probe to measure soil moisture.

Figure 12B. Improved ground data instrumentation. Aerial tramway to collect solar radiation and emission data continuously over the trees.

Figure 12C. Improved ground data instrumentation. Data logger digitizes and records 38 channels of biophysical data.

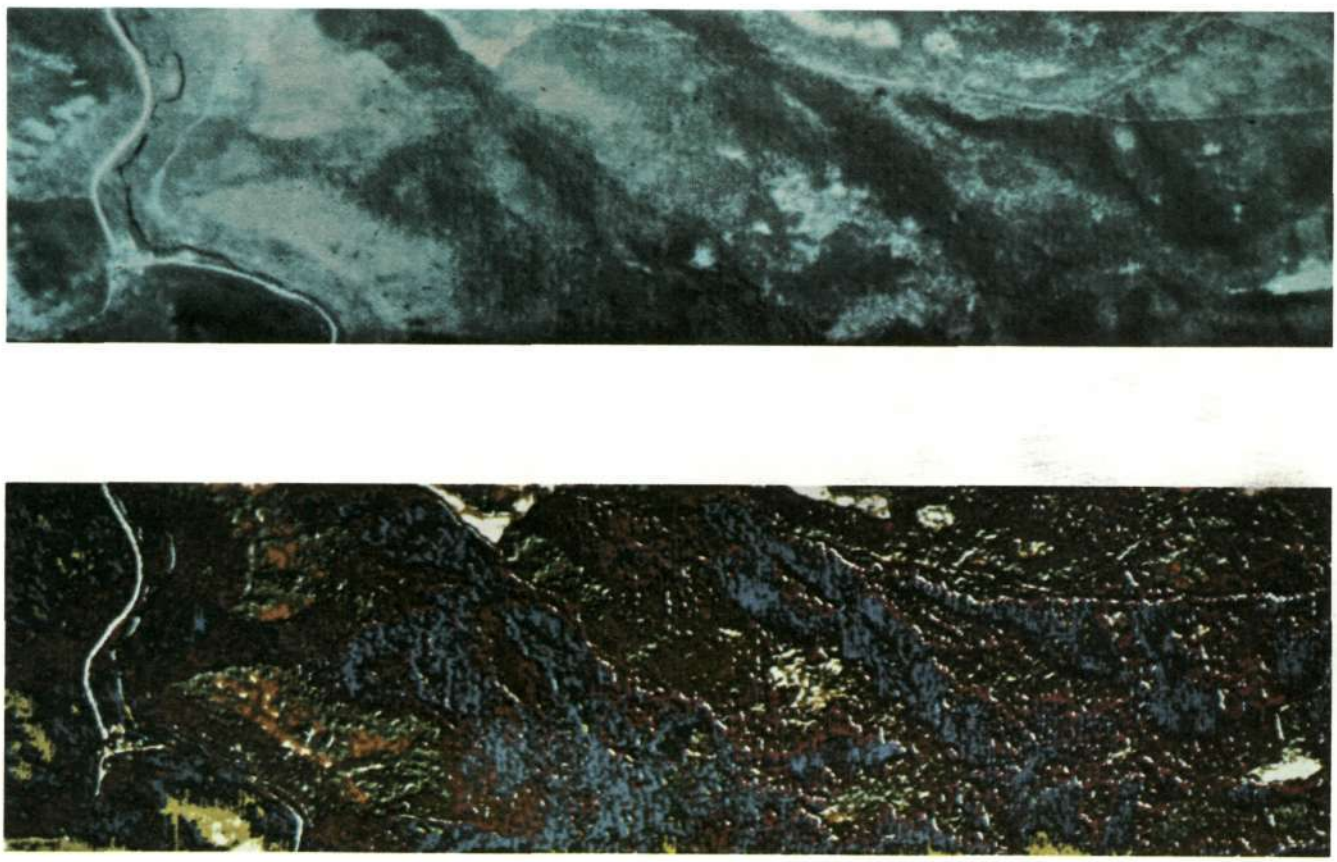

Figure 13.--(A) Black and white analog at top of study area. (B) Thermal contouring from 8.0 - 13.5 micrometer waveband, 1,500 meters above terrain; targets are coded according to small temperature differences.

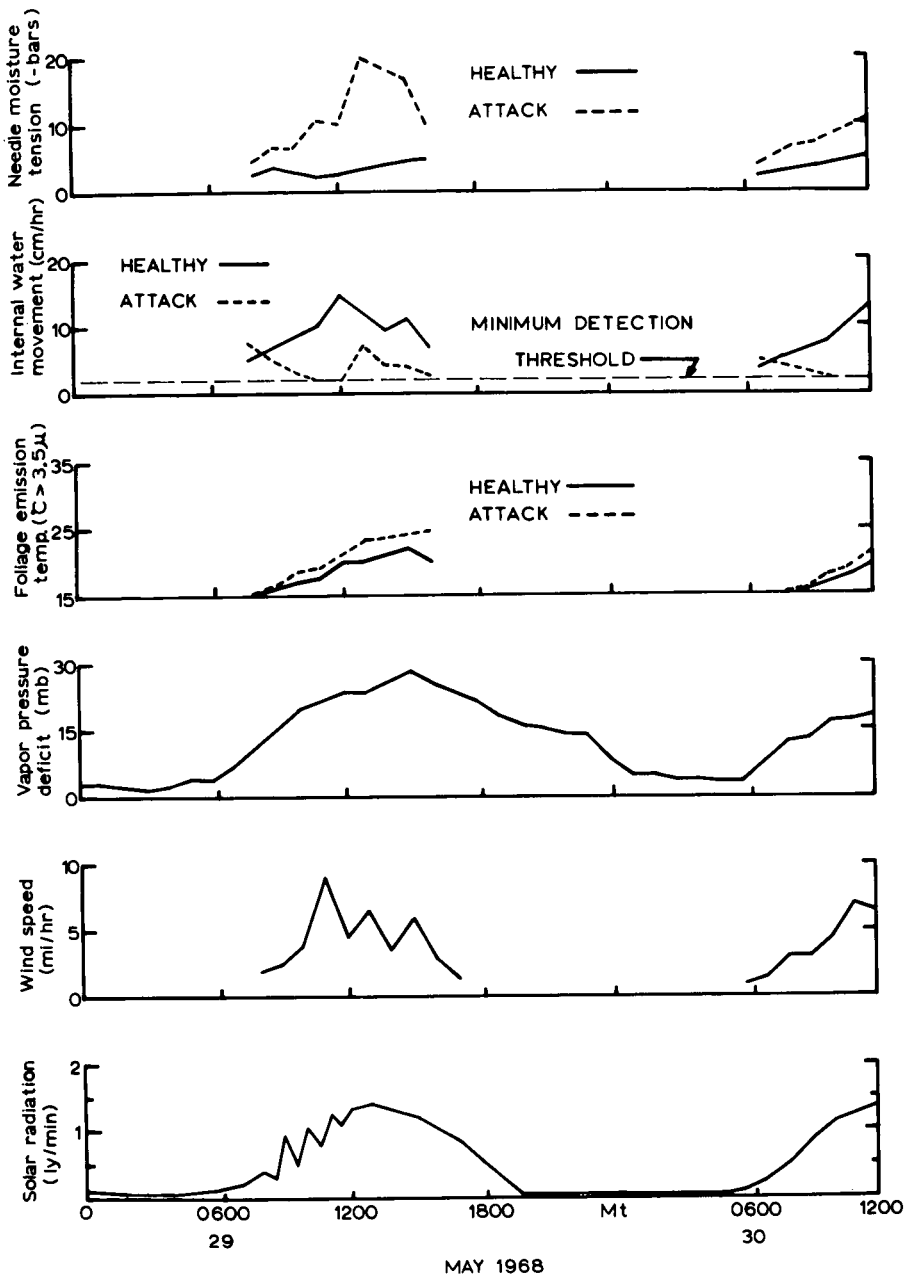

Figure 14.--Meteorological and tree physiological data collected at ground instrumented test site for period May 29 to 30, 1968. Note clear-cut apparent scene radiance difference during period when overflights were made by Michigan C-47 aircraft equipped with multispectral scanner.

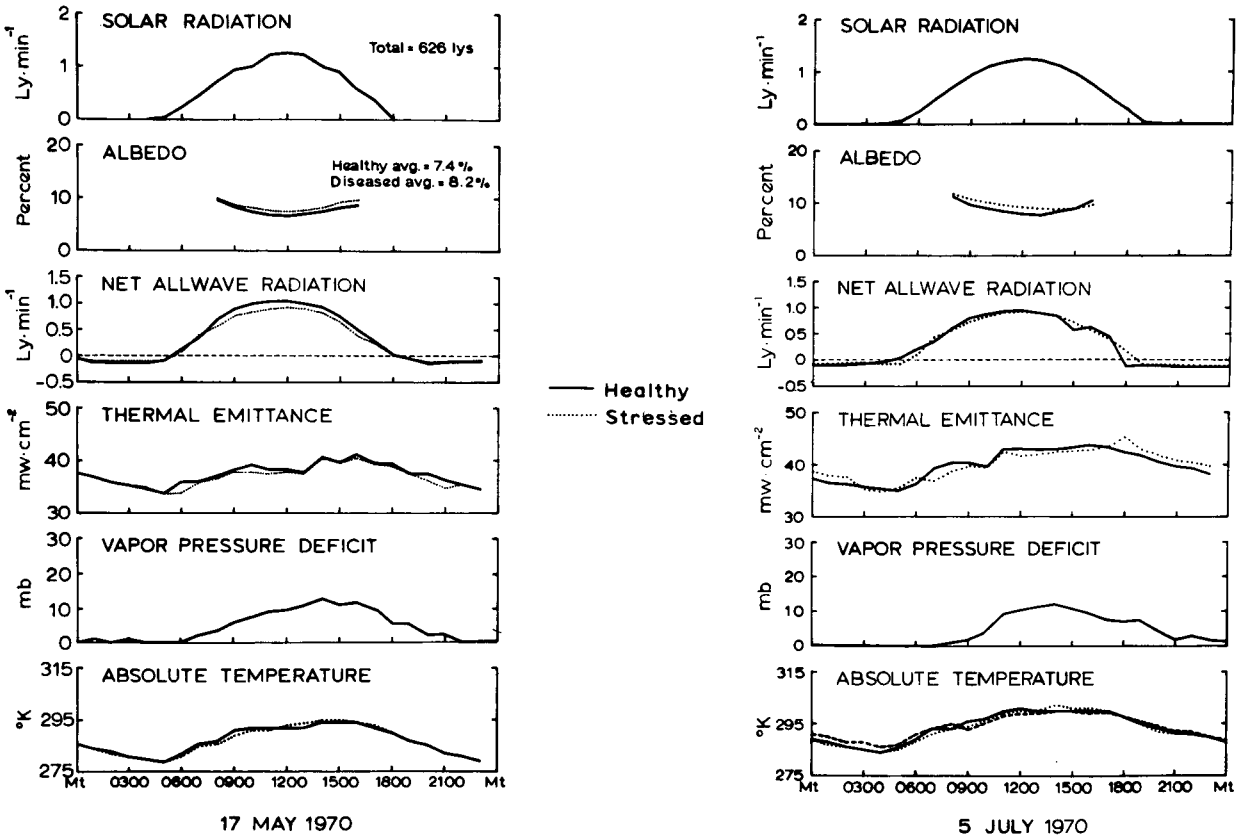

Figure 15.--Ground data collected at *Poria weirii* site on two dates at Wind River, Washington. Compare the thermal radiance graphs with those shown in Figure 14. No apparent scene radiance difference showed up on disease-infected trees as compared with insect-infested trees.

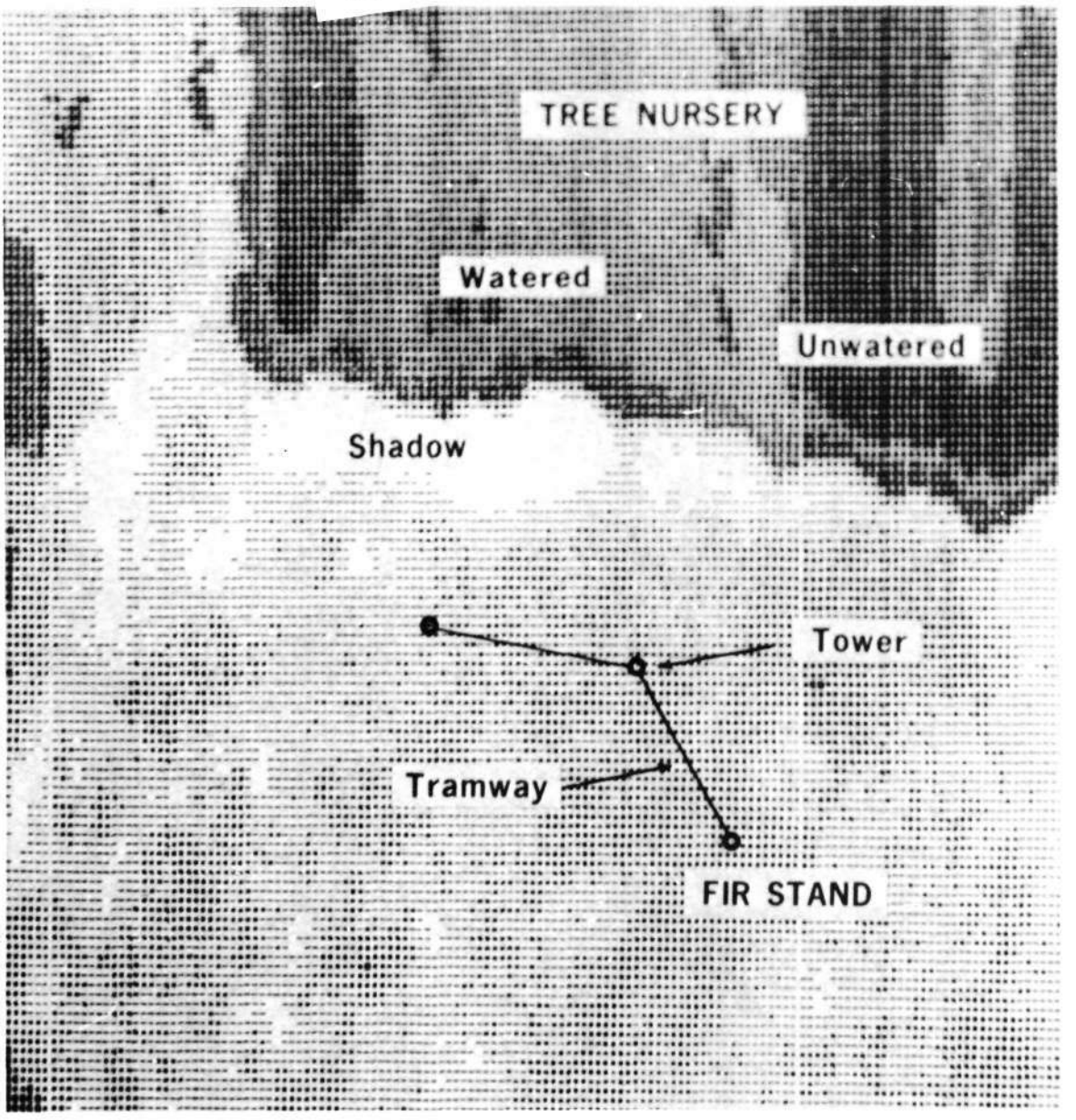

Figure 16.--Thermal gray map of *Poria weirii* site constructed from digitized thermal analog tapes. Data originated from University of Michigan multispectral scanner. No density printout difference occurs around known healthy or infected trees. Warm objects appear dark on this printout.